applied sciences

MDPI

Article

Image-Based Musculoskeletal Models to Accurately Reproduce a Maximum Voluntary Isometric Contraction Test In Silico

Francesca Bottin, Marco Viceconti * and Giorgio Davico

Department of Industrial Engineering, Alma Mater Studiorum—University of Bologna (IT), 40136 Bologna, Italy; francesca.bottin2@unibo.it (F.B.)

* Correspondence: marco.viceconti@unibo.it

Abstract: Musculoskeletal models and computational simulations are increasingly employed in clinical and research settings, as they provide insights into human biomechanics by estimating quantities that cannot be easily measured in vivo (e.g., joint contact forces). However, their clinical application remains limited by the lack of standardized protocols for developing personalized models, which in turn heavily rely on the modeler's expertise and require task-specific validation. While motor tasks like walking and cycling have been widely studied, simulating a maximal knee extensor dynamometry test remains unexplored, despite its relevance in rehabilitation. This study aims to fill this gap by investigating the minimum amount of experimental data required to accurately reproduce a maximal voluntary contraction test in silico. For nine healthy young females, four different subject-specific musculoskeletal models with increasing levels of personalization were developed by incorporating muscle volume data from medical images and electromyographic signal envelopes to adjust, respectively, muscle maximal isometric force and tetanic activation limits. At each step of personalization, simulation outcomes were compared to experimental data. Our findings suggest that to reproduce in silico accurately the isometric dynamometry test requires information from both medical imaging and electromyography, even when dealing with healthy subjects.

Keywords: computational simulations; knee joint in extension; maximum voluntary isometric contraction test; musculoskeletal modeling; personalized muscle properties

Citation: Bottin, F.; Viceconti, M.; Davico, G. Image-Based Musculoskeletal Models to Accurately Reproduce a Maximum Voluntary Isometric Contraction Test In Silico. *Appl. Sci.* **2024**, *14*, 8678. https://doi.org/10.3390/app14198678

Academic Editors: Seyyed Hamed Hosseini Nasab and Renate List

Received: 29 August 2024
Revised: 19 September 2024
Accepted: 24 September 2024
Published: 26 September 2024

1. Introduction

Over the last two decades, the use of musculoskeletal (MSK) dynamics models has increased enormously [1] in their ability to estimate biomechanical quantities that may not be readily measured in vivo (e.g., joint contact forces [2,3]) and supporting clinical-decision making [4,5]. MSK models, often referred to as digital twins, have been generated to simulate various human movements and predict clinical outcomes, e.g., to address orthopedic research questions [6,7], design personalized therapy regimens and rehabilitation programs [8], or enhance athletic performance [9]. Despite their promising applications, their actual clinical application is rarely reported [4,10], because several challenges hinder the widespread adoption of MSK models in clinical practice. For instance, despite the availability of software and workflows to streamline and standardize model development [11,12], the process to generate a personalized MSK model remains time-consuming (i.e., hours—or even days—are required particularly for the segmentation of the bone/muscle geometries instead of few minutes to scale a generic model) and requires a large volume of data, including medical imaging for each subject. Moreover, a unified approach to develop personalized models is lacking, resulting in large variability in terms of MSK model personalization among centers/groups, which is tightly linked to the amount of available experimental data (or lack thereof)—especially in clinical settings. Such variability likely leads to inconsistencies that can affect the reliability and reproducibility of the models and their estimates [13,14].

Numerous studies indicate that generic models fail to adequately represent both skeletal and muscular properties of individual subjects, even when scaled to the dimensions of the subject under study, leading to inaccurate predictions [15–18]. Subject-specific features (e.g., characteristic angles or rotations) are not captured to the point that generic-scaled bones do not well approximate the real bones [19]. In addition, the muscle properties do not scale linearly with the bones [20]. However, since the absence of a standardized procedure, model personalization is left to the modeler's expertise, which does not build trust in the methodology itself [14,21,22]. One notable example is the variety of methods employed to define maximal isometric force [23–25], the choice of which strongly influences the percentage of successful simulations [26].

Another crucial step before a model can be trusted and considered reliable is its validation, which must be performed for the specific motor task being simulated. Validation requires an appropriate number of samples and involves comparing the results of the simulated task with experimental data (from relevant gold standard measures). Additionally, a sensitivity analysis should be conducted to strengthen the validation, ensuring model robustness and reliability. MSK models have been used to simulate the most disparate locomotor tasks, from overground or level walking [22,27] to running [28,29], cycling movements [30,31], or other sports (e.g., rugby [32]). However, to the best of the authors' knowledge, the maximal voluntary isometric contraction (MVIC) test, commonly used to assess quadriceps muscle strength, has seldom been replicated in silico [33,34]. This gap in the literature highlights the need for a standardized approach to simulate accurately such tests, which are essential for assessing muscle strength and functionality.

The aim of the present study was twofold: (1) to develop a robust pipeline for simulating an MVIC of the knee extensors with the future prospect of validation, and (2) to identify the minimum amount of information required to obtain physiologically plausible estimates of the MVIC torque, with a predictive error lower than the intrinsic error of the experimental measurements [35–37]. The main hypothesis was that the measurements extracted from medical images alone would have been sufficient to achieve an acceptable prediction error, for a cohort of healthy subjects, even without informing the model/simulation with the muscle activation levels (computed from the electromyography, EMG, recordings). The results of this work highlighted that both the muscle volumes and activation are necessary to accurately reproduce in silico an MVIC test of the knee extensors. Moreover, to minimize the modeler's influence, the generation of the personalized MSK models followed previously defined and validated model generation steps, and a sensitivity analysis was conducted to account for the uncertainties associated with the only input dependent on the modeler's expertise (i.e., muscle segmentation).

2. Materials and Methods

For this study, both anatomical and experimental data were acquired from ten healthy female adults (Table 1; age—30.7 $\pm$ 5.3 years; height—162 $\pm$ 4.9 cm; weight—54 $\pm$ 5 kg; BMI—20.6 $\pm$ 1.7 kg/m^2). All the volunteers signed informed consent before participating in the study, in accordance with the local Ethical Committee approval (CE AVEC: 216/2020/Sper/IOR, Clinical Trials ID: NCT05091502). The experimental data include full lower limb MRI data, dynamometry, and surface EMG data recorded during an MVIC test with the hip and knee flexed at 90°.

Data from one of the participants (Female 10) were not considered for the analysis as the subject did not perform maximal contractions due to the fear of getting hurt.

Table 1. Subjects data: age, height, mass, body mass index (BMI), and physical activity. * Participant excluded from the study.

Subject	Age (Years)	Height (cm)	Mass (kg)	BMI (kg/m^2)	Physical Activity Level [1]
Female 1	27	170	56	19	3
Female 2	26	158	52	21	2
Female 3	39	167	53	19	3
Female 4	38	166	66	23	3
Female 5	33	155	50	21	3
Female 6	28	158	55	22	3
Female 7	29	160	50	20	3
Female 8	26	165	49	18	3
Female 9	25	158	52	21	3
Female 10 *	36	163	57	21	2

[1] 1—sedentary; 2—some physical activity; 3—regular physical activity and training; 4—regular hard physical training for competition sports.

2.1. MRI Acquisition and Processing

T1-weighted axial MRI scans, from the L3 vertebra to the toes, were acquired on a Discovery TM MR750w 3.0T scanner (GE Healthcare, Chicago, IL, USA) with the following parameters: scanning sequence—proprietary Dixon sequence, slice thickness—3.94 mm, slice increment—2.0 mm, pixel size—0.4688 mm. Depending on the height of each subject, four or five different sections were acquired, with an overlap of at least 40 slices between consecutive sections. The MRI acquisition lasted around 20/30 min. The selected scan allowed for a reduction in the acquisition time minimizing the motion artifacts while maintaining high-quality images essential for enabling semi-automatic segmentation. The images were imported into Mimics v25 (Mimics Innovation Suite, Materialise, Leuven, Belgium) and merged to obtain the entire volume of interest (full lower limbs) in a single file. Within Mimics, a single expert operator manually or semi-automatically segmented bones, muscles, and soft tissues. In particular, the lower limb muscles were segmented employing an atlas-based approach, namely the muscle segmentation tool (MST), that takes in input masks including the whole muscle tissue of a specific section (i.e., upper or lower leg) and gives as output individual muscle masks. A final manual post-processing was performed to refine the 3D volume reconstructions, with particular attention to the knee extensor muscles (i.e., rectus femoris (RF), vastus intermedius (VI), vastus lateralis (VL), and vastus medialis (VM)), which were primarily responsible for the experimentally measured maximal torque.

2.2. Experimental Laboratory Protocol

The experimental protocol (Figure 1) was performed a week after the MRI acquisition, in the morning. The whole procedure consisted of a warm-up followed by the MVIC tests. In line with the literature [38–40], the warm-up exercises included a 10-min cycling session on an ergometer, a sit-to-stand-to-sit task, a 10-m walk back and forth, and 8 submaximal MVIC tasks. All MVIC tests were performed with the participant's dominant leg using the COR1 dynamometer chair (OT Bioelettronica, Torino, Italy). The participants were seated on the dynamometer and strapped to the chair to minimize movement of the trunk and leg beside the knee joint with their arms across their chest (Figure 2).

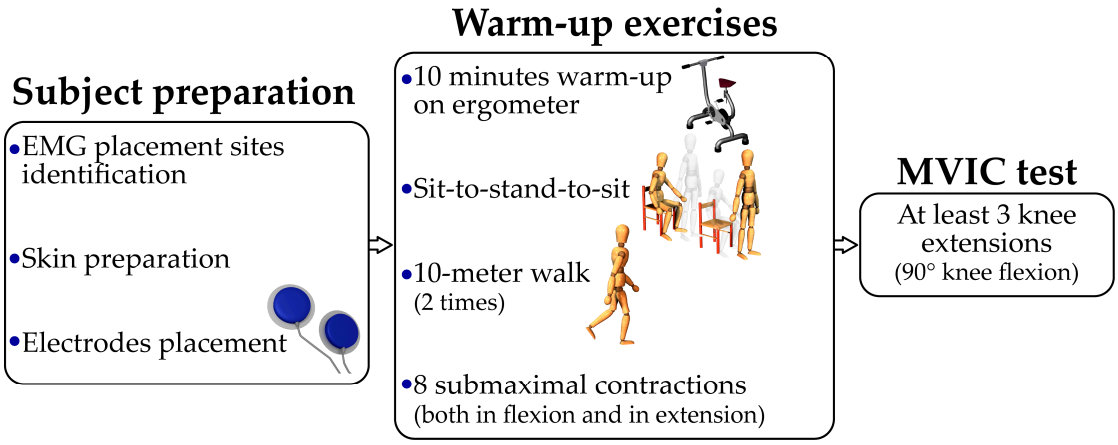

Figure 1. The scheme of the experimental protocol. It includes (1) the preparation of the subject, by identifying and placing the electrodes for the EMG recording, (2) a warm-up on a cycle ergometer and some motor tasks (e.g., 10-m walk), and (3) the MVIC test of the knee flexors and extensors.

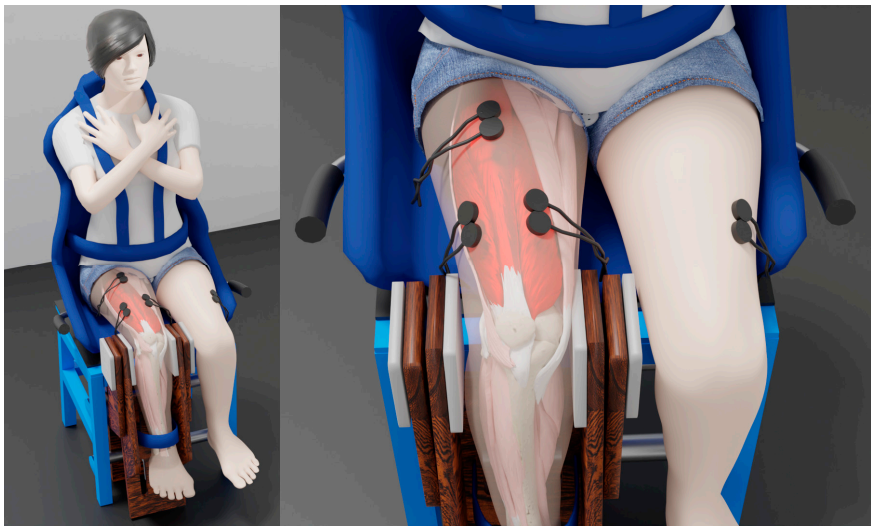

Figure 2. The representation of the experimental setup of the MVIC test of the knee extensors. The subject was placed in a sitting position with the ankle blocked to ensure an isometric position and with each hand on the opposite shoulder throughout the whole test.

The MVIC protocol consisted of the subjects performing three extension contractions, with the knee flexed at 90°. These maximal contractions were to be sustained for approximately 6 s and were separated by 120 s of rest to recover. If the third contraction was higher than the first two, the subject was asked to perform a fourth contraction. During each task, verbal encouragement by the operators and real-time visual feedback of the torque achieved were provided to elicit maximal contractions.

All participants had previously familiarized themselves with the tasks. During the whole protocol, except for the cycle ergometer, EMG signals of eight muscles were registered. In total, the experimental procedure lasted two and a half hours (placement of the EMG electrodes included). In a preliminary study, both the repeatability and reproducibility of the instrumentation were evaluated.

2.3. EMG Recording and Processing

The activity of eight muscles (i.e., rectus femoris, vastus medialis, vastus lateralis, biceps femoris, semitendinosus, and gastrocnemius lateralis of the dominant leg and vastus lateralis and biceps femoris of the contralateral leg) was recorded through bipolar electrodes (Kendall Arbo, servoprax GmbH, Wesel, Germany, 24 mm diameter) connected to a wired

EMG system (Sessantaquattro, OT Bioelettronica, Torino, Italy, at 2000 Hz). An expert operator placed the electrodes following SENIAM recommendations [41]. Due to the nature of the performed test (i.e., MVIC test), the primary focus was on the knee extensors of the tested (and dominant) leg. EMG signals were recorded from the rectus femoris, vastus lateralis, and vastus medialis. As surface EMG was used, it was not possible to record signals from the vastus intermedius. To assess potential co-contraction of the antagonists, EMG signals from the hamstrings (i.e., biceps femoris and semitendinosus) were also recorded. Additionally, the signals from the gastrocnemius of the dominant leg and the vastus lateralis of the non-dominant leg were also recorded to monitor the activity of muscles not directly involved in the test.

The EMG signals were initially filtered using a zero-lag 4th order Butterworth band-pass filter with 20–500 Hz cut-off frequencies [42] and rectified. Then, the root mean squared (RMS) envelopes were extracted using a 500-ms window [43]. Finally, the EMG signals were normalized for each muscle to the maximal value observed across different tasks (i.e., sit-to-stand and MVIC tasks).

2.4. Torque Acquisition and Processing

Dynamometry data were collected by a load cell (TF03, Benewake, Beijing, China: sensitivity—2 mV/V, full scale—100 kg) embedded in the dynamometer. The torque signals were filtered using a zero-lag 4th order Butterworth low pass filter with a 5 Hz cut-off frequency [44]. In order to find the MVIC torques, the 1st derivative of the torque data was computed and the 1000-ms plateau region [45] with the highest mean was defined as the MVIC torque. The plateau was defined as a sequence of 2000 consecutive samples (1000 ms) where the derivative was equal to 0 ($\pm$0.5).

2.5. Subject-Specific Model Generation

From the segmented geometries (i.e., bones, soft tissues, muscles), a single leg subject-specific MSK dynamics model for each participant was developed following the pipeline proposed by Modenese and colleagues [26].

The models, built with the nmsBuilder software (v.2.1) [11], included seven bone complexes linked by idealized joints (i.e., hip, knee, patellofemoral, ankle, subtalar, and metatarsophalangeal joints) for a total of 13 degrees-of-freedom. Joint centers and axes of the reference systems were identified by fitting analytical shapes (i.e., spheres and cylinders) to the articular surfaces, in MeshLab [46]. The patellofemoral joint was defined as in [27]. The inertial properties of each segment (e.g., thigh) were computed from the segmented volumes, assuming the densities of bones and soft tissues to be 1.42 g/cm^3 and 1.02 g/cm^3, respectively [47,48]. Muscle origin and insertion points were taken from a generic atlas (Full Body Model [27]) and mapped onto the subject-specific bony geometries through affine transformations. Wrapping geometries were included to ensure physiological muscle behavior (e.g., to avoid in-bone penetrations) and the line of action of each muscle was checked to fall inside the scanned muscle volume. Minimal manual adjustments were performed where deemed necessary. Each muscle-tendon unit was modeled as a Hill-type actuator [49], described by Millard et al. [50]. The optimal fiber length (OFL) and tendon slack length (TSL) parameters were extracted from the generic Full Body Model and anthropometrically scaled [51]; the maximal isometric force (MIF) values of each muscle were recalculated using the physiological cross-sectional area (PCSA), as per (1) and (2):

$$PCSA_i = V_m^i \cos\theta / l_o, \quad (1)$$

$$MIF_i = \sigma PCSA_i, \quad (2)$$

where V_m is the i-th muscle volume, θ is the pennation angle, l_o the OFL, and σ the specific tension, set at 60 N/cm^2 and in line with literature data [23].

2.6. Muscle Properties Personalization

The base (i.e., less personalized) model, henceforth $M_{genPCSA}$, featured generic MIF values scaled with volumes derived from the linear regression proposed in [23], using the height and mass of the subjects under study.

Lately, by progressively adding the data experimentally collected and processed, three additional models were generated: (1) the M_{ssPCSA} model, which differs from the base model for the MIF values that were defined using subject-specific muscle volumes, segmented from the MRI; (2) the $M_{ssPCSAssEMG}$, an evolution of the M_{ssPCSA} model, where the maximal control for the quadriceps muscles (i.e., RF, VI, VL, and VM) was adjusted (from the default value of 1) based on the EMG data; and (3) the $M_{genPCSAssEMG}$ model, based on the $M_{genPCSA}$ model, with EMG-based maximal activations (as in the $M_{ssPCSAssEMG}$ model). In the last two models, the maximal value of the normalized RMS envelopes of the knee extensors was used to control the activation level of the quadriceps to reflect the experimental data. The activity of the VI muscle, for which experimental data were unavailable, was derived from the VL and VM activations [52,53] as the mean value of their activations. This choice was supported by scientific evidence showing that the three vastii activate similarly and synchronously [54–57]. The difference in the personalization level of the MSK models is summarized in Table 2.

Table 2. Summary of the different personalization steps of the models (ss = subject-specific).

Subject	ss Bones	ss Muscle Volume/Force	ss Muscle Activation Level
$M_{genPCSA}$	V	X	X
M_{ssPCSA}	V	V	X
$M_{ssPCSAssEMG}$	V	V	V
$M_{genPCSAssEMG}$	V	X	V

2.7. Simulation Environment

All models were placed in a sitting position, with the hip and knee flexed at 90°, to mimic the position of the subject on the dynamometer during the MVIC test (Figure 3). Furthermore, to ensure the dynamic consistency of each model, the pelvis motion and the hip coordinates were locked.

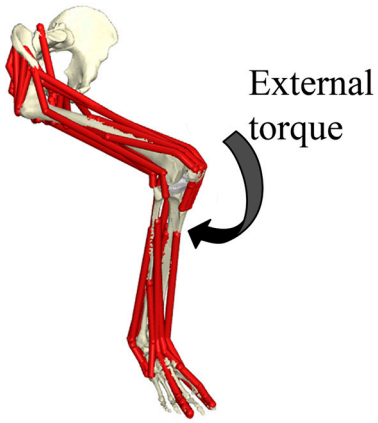

Figure 3. Imposed boundary condition. The single-leg model was placed in a sitting position (90° of hip and knee flexion), while the pelvis and the hip flexion coordinates were locked; the external torque was applied directly at the knee joint.

In OpenSim [58], computer simulations of the MVIC test were performed (1) imposing static kinematics (i.e., the degrees of freedoms in the model were kept constant throughout the whole simulation) and (2) applying constant flexion torque at the knee joint (Figure 3). The external torque was iteratively increased by 1Nm until the forces generated by the

muscles in the model, determined through a static optimization approach that minimized the sum of squared activations (i.e., hypothesizing optimal control), were insufficient to balance them. The last torque value before failure was considered the model's MVIC torque.

2.8. Simulation Framework

The above step/simulation was executed several times, according to the framework described below.

- Initially, the digital twin was informed with average PCSA values, based on healthy adult data ($M_{genPCSA}$). Optimal control was assumed, muscles were allowed to reach a tetanic contraction (maximal activation level equal to 1), and the MVIC torque was predicted.
- If the predicted MVIC torque was much larger than the measured value, the same simulation is performed on the M_{ssPCSA} model, thus accounting for subject-specific PCSA values.
- If, even with the inclusion of patient-specific PCSA values, the digital twin predictions were higher than the experimental values, EMG data collected during the MVIC test were employed to account for non-pathological submaximal activation levels ($M_{ssPCSAssEMG}$).

The $M_{genPCSAssEMG}$ model was finally generated to test whether including personalized muscle activation levels (i.e., without using subject-specific muscle volume segmentations) was enough to simulate the experimental MVIC torque.

2.9. Data Analysis

A Monte Carlo analysis was performed to take into account uncertainties introduced by muscle volume segmentation [59,60], which directly impact the MIF values assigned to the modeled muscles and, in turn, affect the model predictions. Each muscle volume was assumed to be normally distributed, with distinct means and standard deviation. These distributions were calculated to reflect a 5% variability from the reference value determined by the expert operator. An inverse cumulative distribution function was utilized to sample the variables from their respective distributions. Overall, 9000 models (one thousand per subject) were generated, varying the maximal isometric force of each muscle, and employed to perform the in silico MVIC test. The maximal torque obtained simulating the MVIC test with all the models was then compared with the experimental data, to quantify the effect of the uncertainties of the input on the predictions.

As statistical analysis, Pearson correlation and Friedman tests have been performed. The non-parametric statistical Friedman test [61,62] was conducted despite the limited sample size to determine whether the differences in results across various models were statistically significant.

3. Results

Using the base model ($M_{genPCSA}$) resulted in a mean relative error of around 25% (Figure 4). The error was substantially reduced (approximately 15%) when a second level of personalization was introduced (exploiting the MRI or EMG data), with no particular distinctions between the M_{ssPCSA} and the $M_{genPCSAssEMG}$ models. A greater relative error reduction (to 5%) was observed when both anthropometric measurements and subject-specific muscle activations were used (the $M_{ssPCSAssEMG}$).

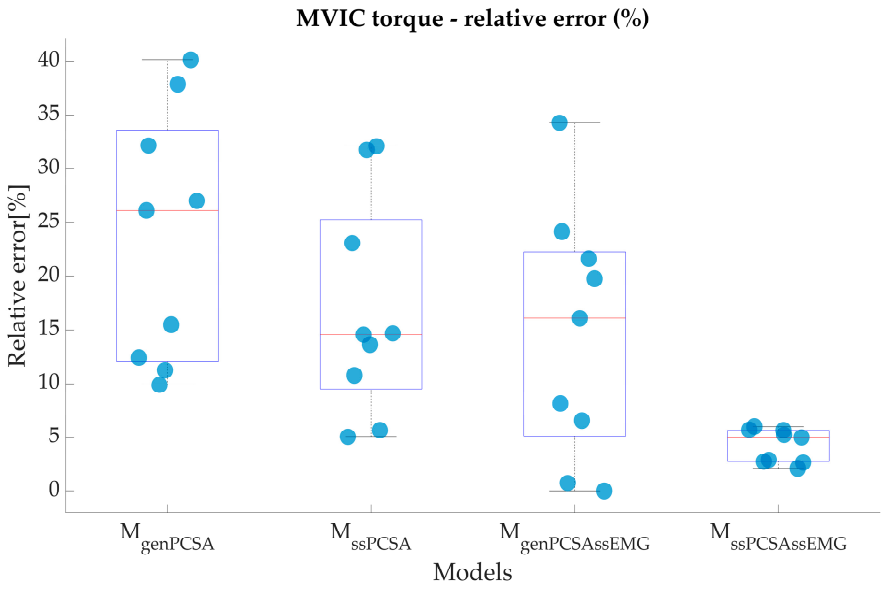

Figure 4. The box plot shows the relative error obtained by comparing the simulation outcomes with the experimentally measured values of the MVIC torque for all four MSK models that are differently personalized.

At a subject level (Figure 5), the $M_{genPCSA}$ model approximated the experimental data only for one out of nine subjects (Figure 5a, subject 7). Using segmented muscle volumes to further tune the MIF values resulted in a more apparent reduction in the simulated extension torque, which more closely approximated the measured values. The above was not true for subjects 6 and 8, for whom the M_{ssPCSA} model predicted an MVIC torque further from the experimental data than the $M_{genPCSA}$ (Figure 5b). The additional use of EMG data ($M_{ssPCSAssEMG}$), more specifically to limit the maximum activation levels of quadriceps muscle, enabled to improve the predictions, which well approximated the experimental values: for all the nine subjects, the $M_{ssPCSAssEMG}$ model was able to predict the experimental MVIC torque within 6%.

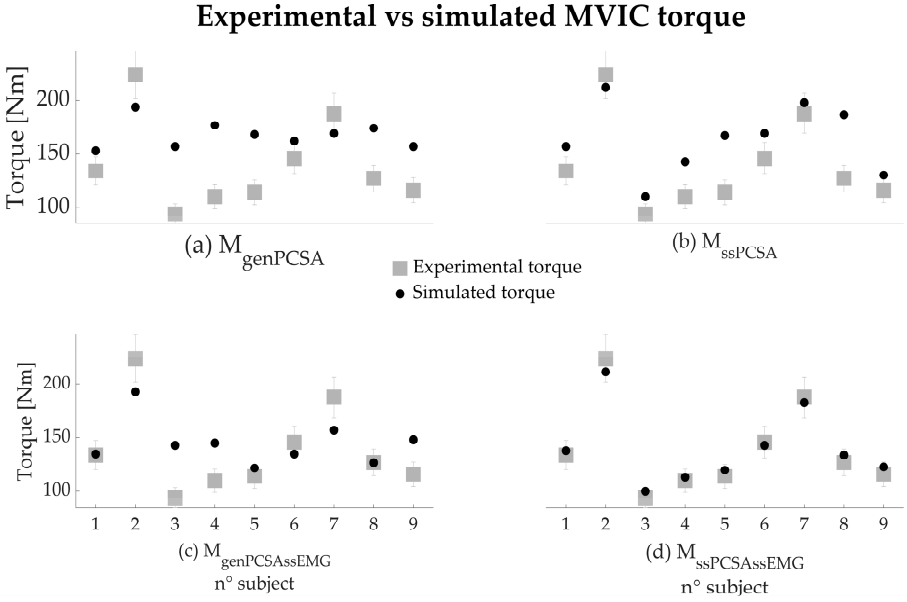

Figure 5. The one-to-one comparison between the maximal torque predicted by the real data (blue square) and the simulation outcomes (purple dot) is provided for the nine healthy female subjects using the four different models: (**a**) $M_{genPCSA}$, (**b**) M_{ssPCSA}, (**c**) $M_{genPCSAssEMG}$, and (**d**) $M_{ssPCSAssEMG}$.

Last, using $M_{genPCSAssEMG}$ models, the error remained high. Only the models of four out of nine subjects predicted a maximal torque with a predictive error within 10% of the corresponding real data.

Data Analysis

The Monte Carlo analysis showed that the model estimates are not significantly affected by segmentation errors in the order of 5% (of the total muscle volume). For all subjects but two, the predicted maximal torques always fell within the set acceptable error range (±10% of experimental data) (Figure 6). Of note, for subjects three and five, only a minimal portion of the 1000 outputs (less than 0.5%) could not be considered accurate enough.

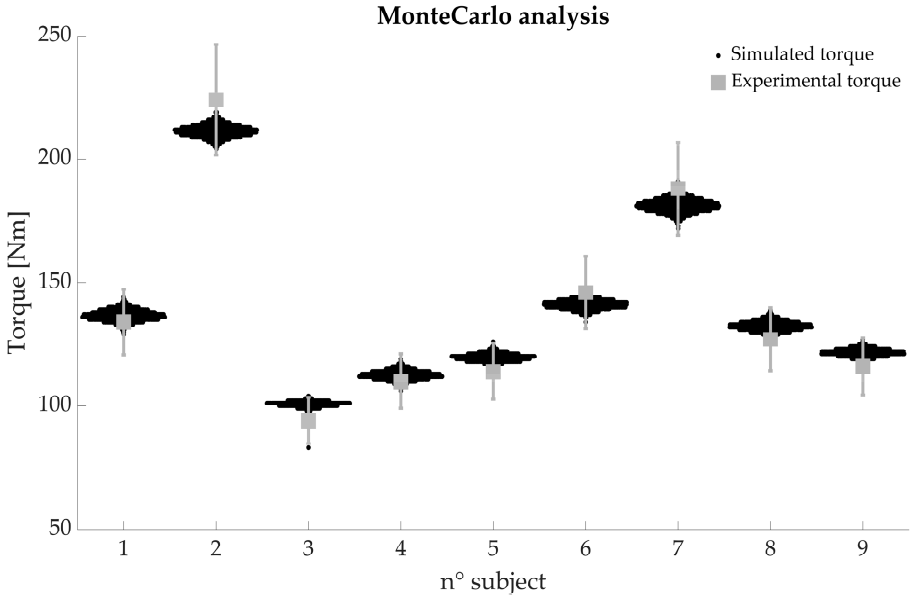

Figure 6. Results from the Montecarlo analysis: the orange dots represent the thousand simulated outcomes for each subject, while the black squares represent the experimental data with the standard deviation error of the dynamometry measurements.

There was a significant correlation only between the $M_{ssPCSAssEMG}$ and M_{ssPCSA} (r = 0.87). On the contrary, for all the other models the Pearson correlation coefficient was lower than 0.8 (with minimum correlation coefficient—r = 0.41—between M_{ssPCSA} and $M_{genPCSAssEMG}$). Finally, given a significance level of 0.05, the *p*-value of 0.014 demonstrates statistical significance between the MSK models with increasing levels of personalization.

4. Discussion

The purpose of this study was (1) to develop a modeling and simulation framework to replicate/conduct an MVIC test in silico by using a combination of experimental data (i.e., EMG recordings, dynamometry data, and medical images) and computational tools (i.e., personalized MSK models) and (2) to identify the minimum level of personalization required to achieve sufficiently accurate predictions (within 10% from the experimentally measured values) in healthy female subjects. To minimize the influence of the modeler in the generation of the personalized MSK model, established procedures, already developed, tested, and validated, were adopted [11,63–66]. In addition, a sensitivity analysis was performed to account for uncertainties of the only personalized input highly influenced by the modeler's expertise (i.e., the segmentations of the muscles).

Four MSK models with varying levels of personalization were built from MRI data for nine healthy young females. The muscle properties were adjusted based on generic muscle volumes representative of an age-matched population (i.e., $M_{genPCSA}$), PCSAs from

medical imaging data (M_{ssPCSA}), the muscle maximum activation level ($M_{genPCSAssEMG}$), or both the PCSAs and the muscle maximum activation level ($M_{ssPCSAssEMG}$).

Our results showed that (1) digital twins are able to predict maximal knee extension torques close to the experimental MVIC torque values observed in vivo in a healthy female cohort, and (2) muscle volumes derived from medical images (i.e., segmented muscle volumes to compute MIF values) are not sufficient alone to achieve acceptable results (i.e., prediction error < 10%). Personalized muscle activation levels may be necessary (i.e., the $M_{ssPCSAssEMG}$). Moreover, the sensitivity analysis highlighted that the predicted outcomes are not influenced by the uncertainties that affect the muscle segmentation and, thus, the maximal isometric force of each muscle.

The MVIC torques at 90° of knee extension experimentally acquired were in line with the literature for an age-matched population [67–69], as well as the predicted maximal torque while using all four different models. However, when population data was used to scale the PCSAs of the models, the models tended to overestimate the experimental values, and the prediction error was acceptable only for one of the subjects, thus suggesting that the $M_{genPCSA}$ models lacked subject specificity.

When personalized information from MRI data was employed to tune the MIF values (M_{ssPCSA}), the error was reduced in general, and for three out of nine subjects, it was within the pre-defined threshold value of 10%. This aligns with previous work showing the need for subject-specific information from medical imaging data [16,70]. Nonetheless, only the combined personalization of both MIF values and maximal activation levels (extracted from experimental EMG data) achieved low errors for all participants, contrary to previous findings [33]. When only the EMG data were employed to personalize the models, the prediction error was comparable to the results of the M_{ssPCSA} models.

This study has some limitations. The lack of kinematic data to accurately describe the knee joint motion throughout the execution of the MVIC test forced us to set a static pose. The isometric nature of the test justified the choice, although it is not ideal since the subject moves during the execution of the test, altering the knee flexion angle and causing misalignment between the joint and the dynamometer axes of rotation [71,72]. Moreover, the personalization of the muscle parameters (i.e., OFL and TSL) was limited, potentially impacting the model's behavior by the difficulty of measuring these values in vivo [73] or the need for additional experimental data (e.g., 3D ultrasound [74] or DTI [33]). However, such parameters were optimized to adjust the generic parameters, ensuring that the force-length-velocity relationships of the generic Full Body Model and the ratio between the optimal fiber length and the tendon slack length were maintained [51]. Finally, the selection of the cohort, which included only female subjects, was dictated by the limitations of the instrumentation used (i.e., dynamometer). A preliminary study revealed that the dynamometer provided repeatable measurements for knee extensor maximal torque below 250 Nm, a threshold that male adults can easily exceed.

5. Conclusions

In conclusion, the present study represents the first step in validating MSK models for reproducing the MVIC test of knee extensors in silico. The minimum amount of information required to achieve a one-to-one match between model predictions and experimental data was identified in both the muscle volumes and the activation level scaled based on the EMG signal. To ensure comprehensive validation, two additional steps are necessary: expanding the sample size, including both sexes and employing an isokinetic dynamometer, the gold standard for MVIC testing. Therefore, further analyses and a larger dataset are needed to confirm these preliminary results.

Author Contributions: Conceptualization, F.B., M.V. and G.D.; data curation, F.B. and G.D.; formal analysis, F.B.; investigation, F.B. and G.D.; methodology, F.B., M.V. and G.D.; project administration, M.V. and G.D.; supervision, M.V.; writing—original draft, F.B.; writing—review and editing, M.V. and G.D. All authors have read and agreed to the published version of the manuscript.

Funding: This study was funded by the H2020 project "In Silico World: Lowering barriers to ubiquitous adoption of In Silico Trials" (topic SC1-DTH-06-2020, grant ID 101016503). The project "ForceLoss: differential diagnosis of force loss in fragile elders" funded by the Italian Ministry of Health (Ricerca finalizzata RF-2019-12369960) supported the clinical study.

Institutional Review Board Statement: The study was conducted in accordance with the local Ethical Committee approval (CE AVEC: 216/2020/Sper/IOR, Clinical Trials ID: NCT05091502).

Informed Consent Statement: Informed consent was obtained from all subjects involved in the study.

Data Availability Statement: The data presented in this study are openly available in AMS Acta at 10.6092/unibo/amsacta/7710 (https://amsacta.unibo.it/id/eprint/7710, accessed on 20 May 2024).

Conflicts of Interest: The authors declare no conflicts of interest. The funders had no role in the design of the study; in the collection, analyses, or interpretation of data; in the writing of the manuscript; or in the decision to publish the results.

References

1. Killen, B.A.; Falisse, A.; De Groote, F.; Jonkers, I. In Silico-Enhanced Treatment and Rehabilitation Planning for Patients with Musculoskeletal Disorders: Can Musculoskeletal Modelling and Dynamic Simulations Really Impact Current Clinical Practice? *Appl. Sci.* **2020**, *10*, 7255. [CrossRef]
2. Navacchia, A.; Myers, C.A.; Rullkoetter, P.J.; Shelburne, K.B. Prediction of In Vivo Knee Joint Loads Using a Global Probabilistic Analysis. *J. Biomech. Eng.* **2016**, *138*, 031002. [CrossRef] [PubMed]
3. Walter, J.P.; Korkmaz, N.; Fregly, B.J.; Pandy, M.G. Contribution of Tibiofemoral Joint Contact to Net Loads at the Knee in Gait. *J. Orthop. Res.* **2015**, *33*, 1054–1060. [CrossRef]
4. Fregly, B.J.; Reinbolt, J.A.; Rooney, K.L.; Mitchell, K.H.; Chmielewski, T.L. Design of Patient-Specific Gait Modifications for Knee Osteoarthritis Rehabilitation. *IEEE Trans. Biomed. Eng.* **2007**, *54*, 1687–1695. [CrossRef]
5. Viceconti, M.; Taddei, F.; Van Sint Jan, S.; Leardini, A.; Cristofolini, L.; Stea, S.; Baruffaldi, F.; Baleani, M. Multiscale Modelling of the Skeleton for the Prediction of the Risk of Fracture. *Clin. Biomech.* **2008**, *23*, 845–852. [CrossRef]
6. Pitto, L.; Kainz, H.; Falisse, A.; Wesseling, M.; Van Rossom, S.; Hoang, H.; Papageorgiou, E.; Hallemans, A.; Desloovere, K.; Molenaers, G.; et al. SimCP: A Simulation Platform to Predict Gait Performance Following Orthopedic Intervention in Children With Cerebral Palsy. *Front. Neurorobot.* **2019**, *13*, 54. [CrossRef] [PubMed]
7. Saxby, D.J.; Bryant, A.L.; Modenese, L.; Gerus, P.; Killen, B.A.; Konrath, J.; Fortin, K.; Wrigley, T.V.; Bennell, K.L.; Cicuttini, F.M.; et al. Tibiofemoral Contact Forces in the Anterior Cruciate Ligament–Reconstructed Knee. *Med. Sci. Sports Exerc.* **2016**, *48*, 2195. [CrossRef]
8. Thelen, D.G.; Chumanov, E.S.; Sherry, M.A.; Heiderscheit, B.C. Neuromusculoskeletal Models Provide Insights into the Mechanisms and Rehabilitation of Hamstring Strains. *Exerc. Sport Sci. Rev.* **2006**, *34*, 135. [CrossRef] [PubMed]
9. Dorn, T.W.; Schache, A.G.; Pandy, M.G. Muscular Strategy Shift in Human Running: Dependence of Running Speed on Hip and Ankle Muscle Performance. *J. Exp. Biol.* **2012**, *215*, 1944–1956. [CrossRef]
10. Rajagopal, A.; Kidziński, Ł.; McGlaughlin, A.S.; Hicks, J.L.; Delp, S.L.; Schwartz, M.H. Pre-Operative Gastrocnemius Lengths in Gait Predict Outcomes Following Gastrocnemius Lengthening Surgery in Children with Cerebral Palsy. *PLoS ONE* **2020**, *15*, e0233706. [CrossRef]
11. Valente, G.; Crimi, G.; Vanella, N.; Schileo, E.; Taddei, F. nmsBuilder: Freeware to Create Subject-Specific Musculoskeletal Models for OpenSim. *Comput. Methods Programs Biomed.* **2017**, *152*, 85–92. [CrossRef] [PubMed]
12. Modenese, L.; Renault, J.-B. Automatic Generation of Personalised Skeletal Models of the Lower Limb from Three-Dimensional Bone Geometries. *J. Biomech.* **2021**, *116*, 110186. [CrossRef]
13. Fregly, B.J. A Conceptual Blueprint for Making Neuromusculoskeletal Models Clinically Useful. *Appl. Sci.* **2021**, *11*, 2037. [CrossRef]
14. Rooks, N.B.; Schneider, M.T.Y.; Erdemir, A.; Halloran, J.P.; Laz, P.J.; Shelburne, K.B.; Hume, D.R.; Imhauser, C.W.; Zaylor, W.; Elmasry, S.; et al. Deciphering the "Art" in Modeling and Simulation of the Knee Joint: Variations in Model Development. *J. Biomech. Eng.* **2021**, *143*, 061002. [CrossRef]
15. Gerus, P.; Sartori, M.; Besier, T.F.; Fregly, B.J.; Delp, S.L.; Banks, S.A.; Pandy, M.G.; D'Lima, D.D.; Lloyd, D.G. Subject-Specific Knee Joint Geometry Improves Predictions of Medial Tibiofemoral Contact Forces. *J. Biomech.* **2013**, *46*, 2778–2786. [CrossRef]
16. Kainz, H.; Wesseling, M.; Jonkers, I. Generic Scaled versus Subject-Specific Models for the Calculation of Musculoskeletal Loading in Cerebral Palsy Gait: Effect of Personalized Musculoskeletal Geometry Outweighs the Effect of Personalized Neural Control. *Clin. Biomech.* **2021**, *87*, 105402. [CrossRef] [PubMed]
17. Kainz, H.; Goudriaan, M.; Falisse, A.; Huenaerts, C.; Desloovere, K.; De Groote, F.; Jonkers, I. The Influence of Maximum Isometric Muscle Force Scaling on Estimated Muscle Forces from Musculoskeletal Models of Children with Cerebral Palsy. *Gait Posture* **2018**, *65*, 213–220. [CrossRef]

18. Scheys, L.; Spaepen, A.; Suetens, P.; Jonkers, I. Calculated Moment-Arm and Muscle-Tendon Lengths during Gait Differ Substantially Using MR Based versus Rescaled Generic Lower-Limb Musculoskeletal Models. *Gait Posture* **2008**, *28*, 640–648. [CrossRef]
19. Davico, G.; Pizzolato, C.; Killen, B.A.; Barzan, M.; Suwarganda, E.K.; Lloyd, D.G.; Carty, C.P. Best Methods and Data to Reconstruct Paediatric Lower Limb Bones for Musculoskeletal Modelling. *Biomech. Model. Mechanobiol.* **2020**, *19*, 1225–1238. [CrossRef]
20. Ward, S.R.; Eng, C.M.; Smallwood, L.H.; Lieber, R.L. Are Current Measurements of Lower Extremity Muscle Architecture Accurate? *Clin. Orthop. Relat. Res.* **2009**, *467*, 1074–1082. [CrossRef]
21. Andreassen, T.E.; Laz, P.J.; Erdemir, A.; Besier, T.F.; Halloran, J.P.; Imhauser, C.W.; Chokhandre, S.; Schwartz, A.; Nohouji, N.A.; Rooks, N.B.; et al. Deciphering the "Art" in Modeling and Simulation of the Knee Joint: Assessing Model Calibration Workflows and Outcomes. *J. Biomech. Eng.* **2023**, *145*, 121008. [CrossRef] [PubMed]
22. Conconi, M.; Montefiori, E.; Sancisi, N.; Mazzà, C. Modeling Musculoskeletal Dynamics during Gait: Evaluating the Best Personalization Strategy through Model Anatomical Consistency. *Appl. Sci.* **2021**, *11*, 8348. [CrossRef]
23. Handsfield, G.G.; Meyer, C.H.; Hart, J.M.; Abel, M.F.; Blemker, S.S. Relationships of 35 Lower Limb Muscles to Height and Body Mass Quantified Using MRI. *J. Biomech.* **2014**, *47*, 631–638. [CrossRef] [PubMed]
24. van der Krogt, M.M.; Bar-On, L.; Kindt, T.; Desloovere, K.; Harlaar, J. Neuro-Musculoskeletal Simulation of Instrumented Contracture and Spasticity Assessment in Children with Cerebral Palsy. *J. NeuroEngineering Rehabil.* **2016**, *13*, 64. [CrossRef]
25. van Veen, B.; Montefiori, E.; Modenese, L.; Mazzà, C.; Viceconti, M. Muscle Recruitment Strategies Can Reduce Joint Loading during Level Walking. *J. Biomech.* **2019**, *97*, 109368. [CrossRef]
26. Modenese, L.; Montefiori, E.; Wang, A.; Wesarg, S.; Viceconti, M.; Mazzà, C. Investigation of the Dependence of Joint Contact Forces on Musculotendon Parameters Using a Codified Workflow for Image-Based Modelling. *J. Biomech.* **2018**, *73*, 108–118. [CrossRef]
27. Rajagopal, A.; Dembia, C.L.; DeMers, M.S.; Delp, D.D.; Hicks, J.L.; Delp, S.L. Full-Body Musculoskeletal Model for Muscle-Driven Simulation of Human Gait. *IEEE Trans. Biomed. Eng.* **2016**, *63*, 2068–2079. [CrossRef] [PubMed]
28. Hamner, S.R.; Seth, A.; Delp, S.L. Muscle Contributions to Propulsion and Support during Running. *J. Biomech.* **2010**, *43*, 2709–2716. [CrossRef]
29. Van Hooren, B.; Meijer, K. Dataset of Running Kinematics, Kinetics and Muscle Activation at Different Speeds, Surface Gradients, Cadences and with Forward Trunk Lean. *Data Brief* **2024**, *54*, 110312. [CrossRef]
30. Clancy, C.E.; Gatti, A.A.; Ong, C.F.; Maly, M.R.; Delp, S.L. Muscle-Driven Simulations and Experimental Data of Cycling. *Sci. Rep.* **2023**, *13*, 21534. [CrossRef]
31. Gatti, A.A.; Keir, P.J.; Noseworthy, M.D.; Beauchamp, M.K.; Maly, M.R. Hip and Ankle Kinematics Are the Most Important Predictors of Knee Joint Loading during Bicycling. *J. Sci. Med. Sport* **2021**, *24*, 98–104. [CrossRef] [PubMed]
32. Cazzola, D.; Holsgrove, T.P.; Preatoni, E.; Gill, H.S.; Trewartha, G. Cervical Spine Injuries: A Whole-Body Musculoskeletal Model for the Analysis of Spinal Loading. *PLoS ONE* **2017**, *12*, e0169329. [CrossRef]
33. Charles, J.P.; Grant, B.; D'Août, K.; Bates, K.T. Subject-Specific Muscle Properties from Diffusion Tensor Imaging Significantly Improve the Accuracy of Musculoskeletal Models. *J. Anat.* **2020**, *237*, 941–959. [CrossRef] [PubMed]
34. De Groote, F.; Van Campen, A.; Jonkers, I.; De Schutter, J. Sensitivity of Dynamic Simulations of Gait and Dynamometer Experiments to Hill Muscle Model Parameters of Knee Flexors and Extensors. *J. Biomech.* **2010**, *43*, 1876–1883. [CrossRef] [PubMed]
35. Colombo, R.; Mazzini, L.; Mora, G.; Parenzan, R.; Creola, G.; Pirali, I.; Minuco, G. Measurement of Isometric Muscle Strength: A Reproducibility Study of Maximal Voluntary Contraction in Normal Subjects and Amyotrophic Lateral Sclerosis Patients. *Med. Eng. Phys.* **2000**, *22*, 167–174. [CrossRef]
36. de Araujo Ribeiro Alvares, J.B.; Rodrigues, R.; de Azevedo Franke, R.; da Silva, B.G.C.; Pinto, R.S.; Vaz, M.A.; Baroni, B.M. Inter-Machine Reliability of the Biodex and Cybex Isokinetic Dynamometers for Knee Flexor/Extensor Isometric, Concentric and Eccentric Tests. *Phys. Ther. Sport.* **2015**, *16*, 59–65. [CrossRef]
37. Dirnberger, J.; Wiesinger, H.-P.; Kösters, A.; Müller, E. Reproducibility for Isometric and Isokinetic Maximum Knee Flexion and Extension Measurements Using the IsoMed 2000-Dynamometer. *Isokinet. Exerc. Sci.* **2012**, *20*, 149–153. [CrossRef]
38. Danneskiold-Samsøe, B.; Bartels, E.M.; Bülow, P.M.; Lund, H.; Stockmarr, A.; Holm, C.C.; Wätjen, I.; Appleyard, M.; Bliddal, H. Isokinetic and Isometric Muscle Strength in a Healthy Population with Special Reference to Age and Gender. *Acta. Physiol.* **2009**, *197* (Suppl. 673), 1–68. [CrossRef]
39. Muff, G.; Dufour, S.; Meyer, A.; Severac, F.; Favret, F.; Geny, B.; Lecocq, J.; Isner-Horobeti, M.-E. Comparative Assessment of Knee Extensor and Flexor Muscle Strength Measured Using a Hand-Held vs. Isokinetic Dynamometer. *J. Phys. Ther. Sci.* **2016**, *28*, 2445–2451. [CrossRef]
40. Draganidis, D.; Chatzinikolaou, A.; Avloniti, A.; Barbero-Álvarez, J.C.; Mohr, M.; Malliou, P.; Gourgoulis, V.; Deli, C.K.; Douroudos, I.I.; Margonis, K.; et al. Recovery Kinetics of Knee Flexor and Extensor Strength after a Football Match. *PLoS ONE* **2015**, *10*, e0128072. [CrossRef]
41. Hermens, H.J.; Freriks, B.; Disselhorst-Klug, C.; Rau, G. Development of Recommendations for SEMG Sensors and Sensor Placement Procedures. *J. Electromyogr. Kinesiol.* **2000**, *10*, 361–374. [CrossRef] [PubMed]

42. Merletti, R.; Cerone, G.L. Tutorial. Surface EMG Detection, Conditioning and Pre-Processing: Best Practices. *J. Electromyogr. Kinesiol.* **2020**, *54*, 102440. [CrossRef] [PubMed]
43. Babault, N.; Pousson, M.; Michaut, A.; Ballay, Y.; Hoecke, J.V. EMG Activity and Voluntary Activation during Knee-Extensor Concentric Torque Generation. *Eur. J. Appl. Physiol.* **2002**, *86*, 541–547. [CrossRef]
44. Thompson, B.J. Influence of Signal Filtering and Sample Rate on Isometric Torque–Time Parameters Using a Traditional Isokinetic Dynamometer. *J. Biomech.* **2019**, *83*, 235–242. [CrossRef] [PubMed]
45. Kooistra, R.D.; de Ruiter, C.J.; de Haan, A. Conventionally Assessed Voluntary Activation Does Not Represent Relative Voluntary Torque Production. *Eur. J. Appl. Physiol.* **2007**, *100*, 309–320. [CrossRef]
46. Cignoni, P.; Callieri, M.; Corsini, M.; Dellepiane, M.; Ganovelli, F.; Ranzuglia, G. *MeshLab: An Open-Source Mesh Processing Tool*; The Eurographics Association: Eindhoven, The Netherlands, 2008; ISBN 978-3-905673-68-5.
47. Dumas, R.; Aissaoui, R.; Mitton, D.; Skalli, W.; de Guise, J.A. Personalized Body Segment Parameters from Biplanar Low-Dose Radiography. *IEEE Trans. Biomed. Eng.* **2005**, *52*, 1756–1763. [CrossRef]
48. White, D.R.; Woodard, H.Q.; Hammond, S.M. Average Soft-Tissue and Bone Models for Use in Radiation Dosimetry. *BJR* **1987**, *60*, 907–913. [CrossRef]
49. Zajac, F.E. Muscle and Tendon: Properties, Models, Scaling, and Application to Biomechanics and Motor Control. *Crit. Rev. Biomed. Eng.* **1989**, *17*, 359–411.
50. Millard, M.; Uchida, T.; Seth, A.; Delp, S.L. Flexing Computational Muscle: Modeling and Simulation of Musculotendon Dynamics. *J. Biomech. Eng.* **2013**, *135*, 0210051–02100511. [CrossRef]
51. Modenese, L.; Ceseracciu, E.; Reggiani, M.; Lloyd, D.G. Estimation of Musculotendon Parameters for Scaled and Subject Specific Musculoskeletal Models Using an Optimization Technique. *J. Biomech.* **2016**, *49*, 141–148. [CrossRef]
52. Lloyd, D.G.; Buchanan, T.S. A Model of Load Sharing Between Muscles and Soft Tissues at the Human Knee During Static Tasks. *J. Biomech. Eng.* **1996**, *118*, 367–376. [CrossRef] [PubMed]
53. Lloyd, D.G.; Besier, T.F. An EMG-Driven Musculoskeletal Model to Estimate Muscle Forces and Knee Joint Moments in Vivo. *J. Biomech.* **2003**, *36*, 765–776. [CrossRef]
54. Boccia, G.; Martinez-Valdes, E.; Negro, F.; Rainoldi, A.; Falla, D. Motor Unit Discharge Rate and the Estimated Synaptic Input to the Vasti Muscles Is Higher in Open Compared with Closed Kinetic Chain Exercise. *J. Appl. Physiol.* **2019**, *127*, 950–958. [CrossRef]
55. Martinez-Valdes, E.; Negro, F.; Falla, D.; De Nunzio, A.M.; Farina, D. Surface Electromyographic Amplitude Does Not Identify Differences in Neural Drive to Synergistic Muscles. *J. Appl. Physiol.* **2018**, *124*, 1071–1079. [CrossRef] [PubMed]
56. Mellor, R.; Hodges, P. Motor Unit Synchronization between Medial and Lateral Vasti Muscles. *Clin. Neurophysiol.* **2005**, *116*, 1585–1595. [CrossRef]
57. Sartori, M.; Reggiani, M.; Farina, D.; Lloyd, D.G. EMG-Driven Forward-Dynamic Estimation of Muscle Force and Joint Moment about Multiple Degrees of Freedom in the Human Lower Extremity. *PLoS ONE* **2012**, *7*, e52618. [CrossRef] [PubMed]
58. Delp, S.L.; Anderson, F.C.; Arnold, A.S.; Loan, P.; Habib, A.; John, C.T.; Guendelman, E.; Thelen, D.G. OpenSim: Open-Source Software to Create and Analyze Dynamic Simulations of Movement. *IEEE Trans. Biomed. Eng.* **2007**, *54*, 1940–1950. [CrossRef] [PubMed]
59. Barnouin, Y.; Butler-Browne, G.; Voit, T.; Reversat, D.; Azzabou, N.; Leroux, G.; Behin, A.; McPhee, J.S.; Carlier, P.G.; Hogrel, J.-Y. Manual Segmentation of Individual Muscles of the Quadriceps Femoris Using MRI: A Reappraisal. *J. Magn. Reson. Imaging* **2014**, *40*, 239–247. [CrossRef]
60. Davico, G.; Bottin, F.; Di Martino, A.; Castafaro, V.; Baruffaldi, F.; Faldini, C.; Viceconti, M. Intra-Operator Repeatability of Manual Segmentations of the Hip Muscles on Clinical Magnetic Resonance Images. *J. Digit. Imaging* **2023**, *36*, 143–152. [CrossRef]
61. Friedman, M. The Use of Ranks to Avoid the Assumption of Normality Implicit in the Analysis of Variance. *J. Am. Stat. Assoc.* **1937**, *32*, 675–701. [CrossRef]
62. Friedman, M. A Comparison of Alternative Tests of Significance for the Problem of m Rankings. *Ann. Math. Stat.* **1940**, *11*, 86–92. [CrossRef]
63. Ascani, D.; Mazzà, C.; De Lollis, A.; Bernardoni, M.; Viceconti, M. A Procedure to Estimate the Origins and the Insertions of the Knee Ligaments from Computed Tomography Images. *J. Biomech.* **2015**, *48*, 233–237. [CrossRef] [PubMed]
64. Bennett, K.J.; Pizzolato, C.; Martelli, S.; Bahl, J.S.; Sivakumar, A.; Atkins, G.J.; Solomon, L.B.; Thewlis, D. EMG-Informed Neuromusculoskeletal Models Accurately Predict Knee Loading Measured Using Instrumented Implants. *IEEE Trans. Biomed. Eng.* **2022**, *69*, 2268–2275. [CrossRef] [PubMed]
65. Lerner, Z.F.; DeMers, M.S.; Delp, S.L.; Browning, R.C. How Tibiofemoral Alignment and Contact Locations Affect Predictions of Medial and Lateral Tibiofemoral Contact Forces. *J. Biomech.* **2015**, *48*, 644–650. [CrossRef]
66. Wu, G.; Siegler, S.; Allard, P.; Kirtley, C.; Leardini, A.; Rosenbaum, D.; Whittle, M.; D'Lima, D.D.; Cristofolini, L.; Witte, H.; et al. ISB Recommendation on Definitions of Joint Coordinate System of Various Joints for the Reporting of Human Joint Motion—Part I: Ankle, Hip, and Spine. *J. Biomech.* **2002**, *35*, 543–548. [CrossRef]
67. Yoon, T.S.; Park, D.S.; Kang, S.W.; Chun, S.I.; Shin, J.S. Isometric and Isokinetic Torque Curves at the Knee Joint. *Yonsei Med. J.* **1991**, *32*, 33–43. [CrossRef]
68. Bohannon, R.W.; Kindig, J.; Sabo, G.; Duni, A.E.; Cram, P. Isometric Knee Extension Force Measured Using a Handheld Dynamometer with and without Belt-Stabilization. *Physiother. Theory Pract.* **2012**, *28*, 562–568. [CrossRef] [PubMed]

69. Murray, M.P.; Duthie, E.H.; Gambert, S.R.; Sepic, S.B.; Mollinger, L.A. Age-Related Differences in Knee Muscle Strength in Normal Women. *J. Gerontol.* **1985**, *40*, 275–280. [CrossRef]
70. Scheys, L.; Van Campenhout, A.; Spaepen, A.; Suetens, P.; Jonkers, I. Personalized MR-Based Musculoskeletal Models Compared to Rescaled Generic Models in the Presence of Increased Femoral Anteversion: Effect on Hip Moment Arm Lengths. *Gait Posture* **2008**, *28*, 358–365. [CrossRef]
71. Herzog, W. The Relation between the Resultant Moments at a Joint and the Moments Measured by an Isokinetic Dynamometer. *J. Biomech.* **1988**, *21*, 5–12. [CrossRef]
72. Van Campen, A.; De Groote, F.; Jonkers, I.; De Schutter, J. An Extended Dynamometer Setup to Improve the Accuracy of Knee Joint Moment Assessment. *IEEE Trans. Biomed. Eng.* **2013**, *60*, 1202–1208. [CrossRef] [PubMed]
73. Redl, C.; Gfoehler, M.; Pandy, M.G. Sensitivity of Muscle Force Estimates to Variations in Muscle–Tendon Properties. *Hum. Mov. Sci.* **2007**, *26*, 306–319. [CrossRef] [PubMed]
74. Sartori, M.; Rubenson, J.; Lloyd, D.G.; Farina, D.; Panizzolo, F.A. Subject-Specificity via 3D Ultrasound and Personalized Musculoskeletal Modeling. In *Converging Clinical and Engineering Research on Neurorehabilitation II*; Ibáñez, J., González-Vargas, J., Azorín, J.M., Akay, M., Pons, J.L., Eds.; Springer International Publishing: Cham, Switzerland, 2017; pp. 639–642.